Electronic Supplementary Material (ESI) for Environmental Science: Advances.
This journal is © The Royal Society of Chemistry 2022

Electronic Supplementary Information

Ultra-fast ^{137}Cs sequestration via a layered inorganic indium thioantimonate

Xi Zeng,[ab] Min Zeng,[c] Ping-Wei Cai,[ab] Jun-Hao Tang,[ab] Wen Ma,[ab] Mei-Ling Feng *[ab] and Xiao-Ying Huang [ab]

[a]State Key Laboratory of Structural Chemistry, Fujian Institute of Research on the Structure of Matter, Chinese Academy of Sciences, Fuzhou 350002, P. R. China

[b]University of Chinese Academy of Sciences, Beijing 100049, P. R. China.

[c]Hubei Key Laboratory of Ferro- & Piezoelectric Materials and Devices, Faculty of Physics and Electronic Science, Hubei University, Wuhan 430062, China

E-mail: fml@fjirsm.ac.cn

1. Adsorption equations

The adsorption capacity q_e (mg/g) at equilibrium, distribution coefficient K_d (mL/g) and removal rate R (%), desorption rate D (%), and leaching rate L (%) can be calculated based on equations (S1), (S2), (S3), (S4) and (S5), respectively:

$$q_e = \frac{V}{m}(C_0 - C_e) \qquad (S1)$$

$$K_d = \frac{V(C_0 - C_e)}{m \quad C_e} \qquad (S2)$$

$$R = \frac{(C_0 - C_e)}{C_0} \times 100\% \qquad (S3)$$

$$D = \frac{(C_{elution} \times V_{elution})}{(C_0 - C_e) \times V} \times 100\% \qquad (S4)$$

$$L = \frac{C_A}{C_T} \times 100\% \qquad (S5)$$

where C_0 (mg/L) and C_e (mg/L) are concentrations of Cs^+ (or other metal ions) at the initial state and equilibrium state, respectively. V (mL) is the Cs^+ solution volume, and m (g) is the mass of KIAS. $C_{elution}$ (mg/L) and $V_{elution}$ (mL) are concentration and volume of eluent, respectively. C_A (mg/L) is the actual concentration of In in the solution after soaking the sample, and C_T (mg/L) is the theoretical concentration of In when the sample is completely dissolved in the solution.

Two classical models are commonly used in adsorption kinetic data, namely the pseudo-first-order and pseudo-two-order kinetic models. The integrated pseudo-first-order and seudo-two-order models are expressed using equations (S6) and (S7), respectively.

$$\ln(q_e - q_t) = \ln q_e - k_1 t \qquad (S6)$$

$$\frac{t}{q_t} = \frac{1}{k_2 q_e^2} - \frac{t}{q_e} \qquad (S7)$$

where q_e (mg/g) and q_t (mg/g) are the amounts of Cs^+ ions adsorbed at equilibrium state and at time t, respectively. t (min) is a adsorption time. k_1 (min^{-1}) and k_2 (g/mg min^{-1}) are respectively the rate constants of pseudo-first-order and pseudo-two-order. The

pseudo-two-order model has more complex reaction mechanism than the pseudo-first-order model, which assumes that the adsorption process involves both physical diffusion and chemiadsorption, and that chemiadsorption is the main rate-limiting step.[1]

The main common adsorption isotherm models in solution systems about the initial concentration of Cs^+ adsorbed are the Langmuir and the Freundlich models, which are used to obtain the maximum adsorption capacity (q_m). The linear forms of the two models can be expressed by equations (S8) and (S9), respectively.

$$\frac{C_e}{q_e} = \frac{1}{q_m K_L} + \frac{C_e}{q_m} \qquad (S8)$$

$$\ln q_e = \ln K_F + \frac{1}{n} \ln C_e \qquad (S9)$$

where q_e (mg/g) and q_m (mg/g) are the equilibrium adsorption amount and maximum adsorption capacity, respectively. C_e (mg/L) is the equilibrium concentration of Cs^+ in solution. K_L (L/mg) is the Langmuir constant related to the free energy of adsorption. K_F [(mg/g)(L/mg)$^{1/n}$)] is the Freundlich constant related to the adsorbent capacity. n is the constant indicating the intensity of the adsorption process. The Langmuir model assumes that the adsorption on the solid surface is homogeneous, ideal monolayer adsorption; that all adsorption sites have equal capacity; that the interactions between adjacent sites are ignored; and that there are no mutual forces between adsorbed molecules.[2] The Freundlich model is commonly used to fit the adsorption process to the inhomogeneous surface of a solid. The model assumes that the energy distribution on the adsorbent surface is not homogeneous; that the adsorbent surface sites are occupied by adsorbate and that the energies are ordered from high to low during the adsorption process.[3]

The type of Langmuir model can be evaluated by separation fator (R_L). The adsorption process may be irreversible for $R_L = 0$, favourable for $0 < R_L < 1$, linear for $R_L = 1$, or unfavourable for $R_L > 1$.[4] The definition is as follow:

$$R_L = \frac{1}{1 + K_L C_0} \qquad (S10)$$

where C_0 (mg/L) is the highest initial concentration of Cs^+.

The theoretical adsorption capacity can be calculated based on equation (S11).

$$q(theoretical) = \frac{2 \times atomic\ weight\ of\ Cs}{Formula\ weight\ of\ KIAS} \times 1000 \qquad (S11)$$

2. Characterizations

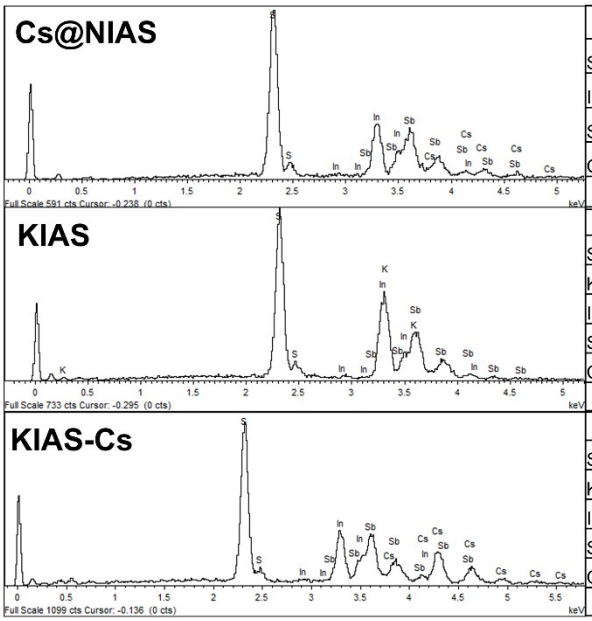

Element	Weight %	Atomic %
S K	28.54	59.84
In L	31.70	18.63
Sb L	28.91	16.03
Cs L	10.85	5.50
Total	100.00	100.00

Element	Weight %	Atomic %
S K	27.54	52.27
K K	9.97	15.51
In L	32.1	17.02
Sb L	30.4	15.2
Cs L	0	0
Total	100.00	100.00

Element	Weight %	Atomic %
S K	24.29	55.1
K K	0	0
In L	25.69	16.27
Sb L	25.18	15.04
Cs L	24.83	13.58
Total	100.00	100.00

Fig. S1. EDS analysis results of Cs@NIAS, KIAS and KIAS-Cs.

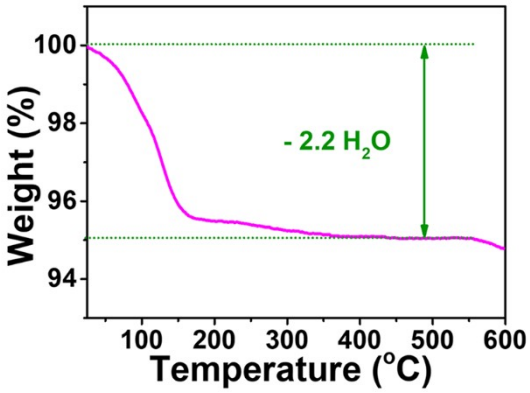

Fig. S2. TGA analysis results of KIAS.

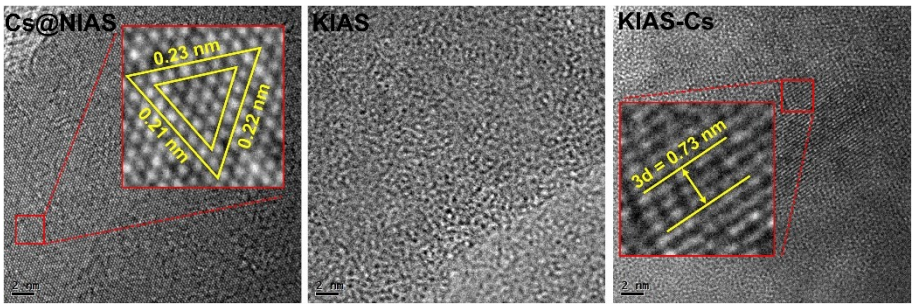

Fig. S3. High-resolution TEM images of Cs@NIAS, KIAS and KIAS-Cs.

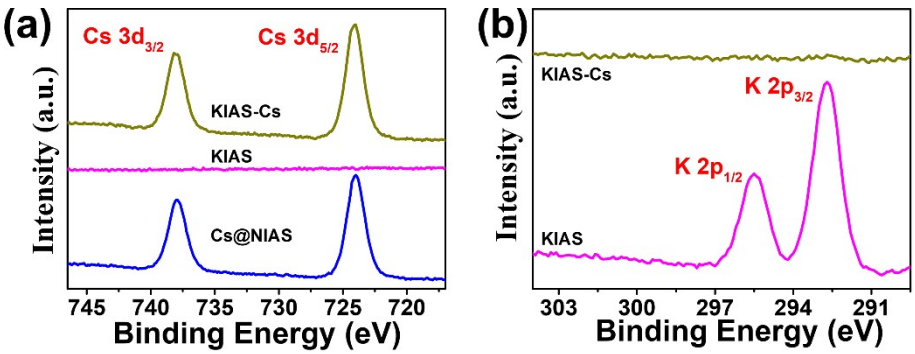

Fig. S4. XPS high-resolution (a) Cs 3d and (b) K 2p spectra of Cs@NIAS, KIAS and KIAS-Cs.

3. Radiolytic and hydrolytic stability

Table S1. Distribution coefficients and removal rates of Cs^+ ions captured by KIAS before and after γ-ray irradiation (V = 10 mL, m = 10 mg, V/m = 1000 mL/g; 5 h contact time; at room temperature).

	C_0^{Cs} (mg/L)	C_e^{Cs} (mg/L)	q^{Cs} (mg/g)	K_d^{Cs} (mL/g)	R^{Cs} (%)
Pristine	7.75	0.183	7.568	4.15×10^4	97.65
100 kGy γ	7.75	0.448	7.303	1.63×10^4	94.23
200 kGy γ	7.75	0.57	7.18	1.26×10^4	92.65
Pristine	41.3	1.345	39.955	2.97×10^4	96.74
100 kGy γ	41.3	1.735	39.565	2.28×10^4	95.80
200 kGy γ	41.3	1.9	39.4	2.07×10^4	95.40

Table S2. The pH-dependent Cs^+ ion-exchange results and In^{3+} leaching rates of KIAS soaked in Cs^+-solutions with different pH values (V = 10 mL, m = 10 mg, V/m = 1000 mL/g; 5 h contact time; at room temperature).

Initial pH	C_0^{Cs} (mg/L)	C_e^{Cs} (mg/L)	q^{Cs} (mg/g)	K_d^{Cs} (mL/g)	R^{Cs} (%)	C^{In} (mg/L)	L^{In} (%)
1.1	4.627	2.58	2.047	7.93×10^2	44.23	0.0210	0.0075
2.2	6.7	3.33	3.37	1.01×10^3	50.30	0.0187	0.0066
3.2	4.437	0.286	4.151	1.45×10^4	93.55	0.0166	0.0059
4.0	4.456	0.345	4.111	1.19×10^4	92.26	0.0280	0.0099
5.4	4.256	0.212	4.044	1.91×10^4	95.02	0.0320	0.0114
6.2	4.304	0.181	4.123	2.28×10^4	95.81	0.0390	0.0138
7.2	4.437	0.188	4.248	2.26×10^4	95.76	0.0240	0.0085
8.1	4.38	0.179	4.201	2.35×10^4	95.92	0.0122	0.0043
9.0	4.475	0.221	4.253	1.92×10^4	95.05	0.0116	0.0041
10.1	4.38	0.199	4.181	2.11×10^4	95.47	0.0129	0.0046
11.1	4.418	0.318	4.099	1.29×10^4	92.80	0.0097	0.0034
12.0	4.076	1.82	2.255	1.24×10^3	55.34	0.0179	0.0064
13.0	5.558	3.11	2.448	7.87×10^2	44.04	0.0168	0.0060

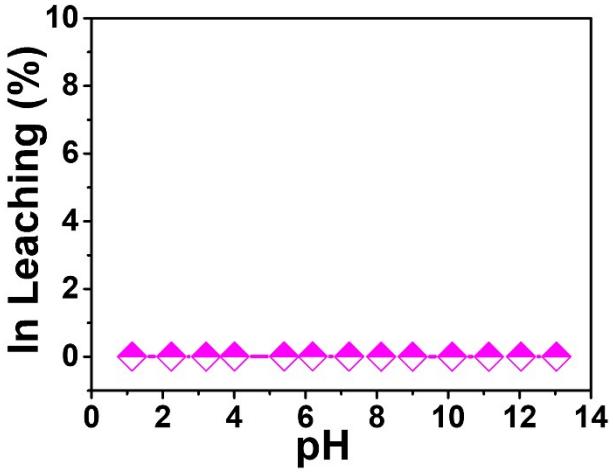

Fig. S5. The In^{3+} leaching rates of KIAS soaked in Cs^+-solutions with different pH values.

4. Adsorption kinetics

Table S3. The adsorption kinetic results of NIAS ($[(CH_3)_2NH_2]_2In_2Sb_2S_7$) towards Cs^+ (V = 50 mL, m = 50 mg, V/m = 1000 mL/g; at room temperature).

Time (minutes)	C_t^{Cs} (mg/L)	q_t^{Cs} (mg/g)	K_d^{Cs} (mL/g)	R^{Cs} (%)
0	1.918	0	0	0
2	1.08	0.838	775.93	43.69
5	1.08	0.838	775.93	43.69
10	1.112	0.806	724.82	42.02
20	1.208	0.71	587.75	37.02
30	1.248	0.67	536.86	34.93
60	1.314	0.604	459.67	31.49
80	1.39	0.528	379.86	27.53
120	1.432	0.486	339.39	25.34
180	1.582	0.336	212.39	17.52
360	1.616	0.302	186.88	15.75
600	1.76	0.158	89.77	8.24

Table S4. The adsorption kinetic results of KIAS towards Cs^+ (V = 50 mL, m = 50 mg, V/m = 1000 mL/g; at room temperature).

Time (minutes)	C_t^{Cs} (mg/L)	q_t^{Cs} (mg/g)	K_d^{Cs} (mL/g)	R^{Cs} (%)
0	2.05	0	0	0
1	0.144	1.906	1.32×10^4	92.98
2	0.11	1.94	1.76×10^4	94.63
5	0.109	1.941	1.78×10^4	94.68
10	0.094	1.956	2.08×10^4	95.41
20	0.081	1.969	2.43×10^4	96.05
30	0.101	1.949	1.93×10^4	95.07
60	0.099	1.951	1.97×10^4	95.17
80	0.097	1.953	2.01×10^4	95.27
120	0.102	1.948	1.91×10^4	95.02
180	0.093	1.957	2.10×10^4	95.46
360	0.099	1.951	1.97×10^4	95.17
600	0.092	1.958	2.13×10^4	95.51

Table S5. Comparison of Cs^+ adsorption performance for KIAS and other adsorbents.

Materials	Temperature	Active pH range	kinetics/R^{Cs}	q_m^{Cs} (mg/g)	Ref.
KIAS	RT	1.1–13.0	1 min/92.98%	309.60	This work
FJSM-GAS-1	RT	NA	NA	164.23	[5]
$[CH_3NH_3]_{20}Ge_{10}Sb_{28}S_{72}\cdot 7H_2O$	65 °C	2.8–11.0	2 min/59%	230.91	[6]
KATS-2	RT	1-12	5 min/99%	358	[7]
FJSM-SnS	65 °C	0.7–11.0	5 min/73%	408.91	[8]
FJSM-SnS-2	RT	3.2–9.3	< 60 min/83.56%	266.54	[9]
FJSM-SnS-3	RT	3.2–9.3	< 60 min/73.36%	109.68	[9]
FJSM-SbS	80 °C	3.4–11.4	2 min/86.90%	143.47	[10]
KMS-1	RT	0.8–11.6	5 min/90%	226	[11]
KMS-2	RT	3–10	10–15 h/NA	531.74	[12]
KTS-3	RT	2–12	5 min/94%	280	[13]
InSnOS	RT	2–12	5 min/97%	537.71	[14]
K@RWY	RT	1.6–11.8	5 min/97%	310	[15]
K-MPS-1	RT	2–12	15 min/78%	337.48	[16]
KMS-1/r-GO	RT	2–13	> 4 h/69%	338.18	[17]
KMS-1/PAN	25 °C	3–11	3 h/< 90%	69.75	[18]
KTS-3/PAN	25 °C	2–12	> 4 h/95%	133.6	[19]
FJSM-InMOF	~25 °C	NA	> 3 h/91.73%	198.63	[20]
MOF/KNiFC	25 °C	2–9	45 min	153	[21]
$K_4Nb_6O_7$	RT	1–14	5 h/50%	166.13	[22]
$Na_2V_6O_{16}\cdot 3H_2O$	RT	NA	10 min/94%	285.75	[23]
NaFeTiO	25 °C	2.1–10.1	200 min/97.5	52.8	[24]
Zeolite A	25 °C	2–8	90 min/90%	207.47	[25]
NaMT1	25 °C	3–11	> 1 h/86.98%	290.70	[26]
AMP-PAN	20 °C	2–10	NA	81.31	[27]

RT = room temperature; NA = Not available.

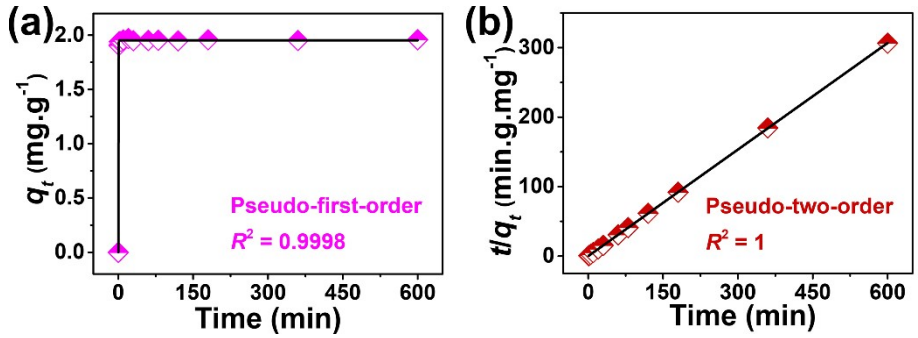

Fig. S6. Kinetics data fitted using (a) pseudo-first-order model and (b) pseudo-second-order model for KIAS.

5. Adsorption isotherms

Table S6. The adsorption isotherm results of KIAS towards Cs^+ (V = 10 mL, m = 10 mg, V/m = 1000 mL/g; 5 h contact time; at room temperature).

C_0^{Cs} (mg/L)	C_e^{Cs} (mg/L)	q^{Cs} (mg/g)
76.75	9	67.75
111.875	18.75	93.125
120	19.375	100.625
210.875	50.375	160.5
293.75	106.375	187.375
413.75	170.5	243.25
522.5	265	257.5
576.25	307.5	268.75
642.5	361.25	281.25
787.5	502.5	285

6. Effects of coexisting ions and dissolved organic matter

Table S7. The results for the Cs^+-exchange of KIAS with individual competitive alkali or alkali-earth ions (V = 10 mL, m = 10 mg, V/m = 1000 mL/g; 5 h contact time; at room temperature).

Cation species	C_0^{Cs} (mg/L)	C_e^{Cs} (mg/L)	q^{Cs} (mg/g)	K_d^{Cs} (mL/g)	R^{Cs} (%)
35.69 mg/L Na^+	3.87	0.273	3.597	1.32×10^4	92.95
41.49 mg/L K^+	3.53	0.28	3.25	1.16×10^4	92.07
43.1 mg/L Rb^+	3.31	0.198	3.113	1.58×10^4	94.03
38.14 mg/L Mg^{2+}	4.525	0.393	4.132	1.05×10^4	91.31
38.51 mg/L Ca^{2+}	3.195	0.305	2.89	9.48×10^3	90.45
48.54 mg/L Sr^{2+}	3.953	0.975	2.978	3.05×10^3	75.33
24.44 mg/L Ba^{2+}	4.328	0.36	3.968	1.10×10^4	91.68

Table S8. The results for the Cs^+-exchange of KIAS with competitive excess Na^+ ions from NaCl (V = 10 mL, m = 10 mg, V/m = 1000 mL/g; 5 h contact time; at room temperature).

Initial Na/Cs molar ratio	C_0^{Na} (mg/L)	C_0^{Cs} (mg/L)	C_e^{Cs} (mg/L)	q^{Cs} (mg/g)	K_d^{Cs} (mL/g)	R^{Cs} (%)
12.43	11.764	5.47	0.326	5.144	1.58×10^4	94.04
53.31	35.69	3.87	0.273	3.597	1.32×10^4	92.95
300.78	148.8	2.86	0.906	1.954	2.16×10^3	68.32
916.94	467.9	2.95	1.883	1.067	5.67×10^2	36.17
16779.11	11725.8	4.04	3.21	0.83	2.59×10^2	20.54

Table S9. The results for the Cs^+-exchange of KIAS with competitive excess Sr^{2+} ions from $SrCl_2$ (V = 10 mL, m = 10 mg, V/m = 1000 mL/g; 5 h contact time; at room temperature).

Initial Sr/Cs molar ratio	C_0^{Sr} (mg/L)	C_0^{Cs} (mg/L)	C_e^{Cs} (mg/L)	q^{Cs} (mg/g)	K_d^{Cs} (mL/g)	R^{Cs} (%)
0.66	1.92	4.443	0.155	4.288	2.77×10^4	96.51
1.91	5.15	4.08	0.478	3.603	7.54×10^3	88.30
18.63	48.54	3.953	0.975	2.978	3.05×10^3	75.33
67.78	194.6	4.355	3.093	1.263	4.08×10^2	28.99
190.95	474.9	3.773	3.015	0.758	2.51×10^2	20.08

Table S10. The results for the Cs^+-exchange of KIAS in the presence of interfering anions (V = 10 mL, m = 10 mg, V/m = 1000 mL/g; 5 h contact time; at room temperature).

Anion species	C_0^{Cs} (mg/L)	C_e^{Cs} (mg/L)	q^{Cs} (mg/g)	K_d^{Cs} (mL/g)	R^{Cs} (%)
30 mg/L CO_3^{2-}	5.006	0.451	4.555	1.01×10^4	90.99
30 mg/L HCO_3^-	5.464	0.231	5.234	2.27×10^4	95.78
30 mg/L NO_3^-	5.127	0.414	4.713	1.14×10^4	91.93
30 mg/L SO_4^{2-}	5.104	0.299	4.805	1.61×10^4	94.14

Table S11. The results for the Cs^+-exchange of KIAS in the presence of interfering humic acid (V = 10 mL, m = 10 mg, V/m = 1000 mL/g; 1−10 mg/L humic acid as dissolved organic matter; 5 h contact time; at room temperature).

HA (mg/L)	C_0^{Cs} (mg/L)	C_e^{Cs} (mg/L)	q^{Cs} (mg/g)	K_d^{Cs} (mL/g)	R^{Cs} (%)
0.5	4.414	0.092	4.323	4.72×10^4	97.93
1	4.426	0.082	4.344	5.28×10^4	98.14
2	4.700	0.089	4.611	5.18×10^4	98.11
5	4.744	0.100	4.644	4.63×10^4	97.89
10	4.696	0.096	4.601	4.80×10^4	97.96

7. Cs^+ ions capture in actual water environments

Table S12. The results of Cs^+-adsorption for KIAS in tap water and lake water (V = 10 mL, m = 10 mg, V/m = 1000 mL/g; 5 h contact time; at room temperature).

Experimental condition	Mixed ions	C_0 (mg/L)	C_e (mg/L)	q (mg/g)	K_d (mL/g)	R (%)
Tap water	Cs^+	7.35	1.03	6.32	6.14×10^3	85.99
	Na^+	19.649	17.681	1.968	111.31	10.02
	K^+	4.001	48.25	-44.249	-917.08	-1105.95
	Mg^{2+}	2.036	1.21	0.826	682.64	40.57
	Ca^{2+}	14.498	8.054	6.444	800.10	44.45
Lake water	Cs^+	5.8	0.73	5.07	6.95×10^3	87.41
	Na^+	13.751	11.708	2.043	174.50	14.86
	K^+	3.624	41.27	-37.646	-912.19	-1038.80
	Mg^{2+}	1.743	0.989	0.754	762.39	43.26
	Ca^{2+}	12.576	7.06	5.516	781.30	43.86

8. Desorption and regeneration

Table S13. The results of five consecutive adsorption-desorption recycling experiments for KIAS (V = 10 mL, m = 10 mg, V/m = 1000 mL/g; 5 h contact time; at room temperature).

Cycles	C_0^{Cs} (mg/L)	C_e^{Cs} (mg/L)	q^{Cs} (mg/g)	K_d^{Cs} (mL/g)	R^{Cs} (%)	C^{In} (mg/L)	L^{In} (%)	$C_{elution}{}^{Cs}$ (mg/L)	D^{Cs} (%)
1	7.152	0.566	6.586	1.16×10^4	92.09	0.0464	0.0165	6.242	94.78
	53.016	2.972	50.044	1.68×10^4	94.39	0.0439	0.0156	47.702	95.32
2	7.152	0.624	6.528	1.05×10^4	91.28	0.0174	0.0062	6.364	97.49
	53.016	4.758	48.258	1.01×10^4	91.03	0.0066	0.0023	46.406	96.16
3	7.152	0.546	6.606	1.21×10^4	92.37	0.0257	0.0091	6.362	96.31
	53.016	2.69	50.326	1.87×10^4	94.93	0.0211	0.0075	48.522	96.42
4	7.152	0.602	6.55	1.09×10^4	91.58	0.0181	0.0064	6.418	97.98
	53.016	3.226	49.79	1.54×10^4	93.92	0.0176	0.0062	46.54	93.47
5	7.152	0.604	6.548	1.08×10^4	91.55	0.0093	0.0033	6.218	94.96
	53.016	3.978	49.038	1.23×10^4	92.50	0.0108	0.0038	47.468	96.80

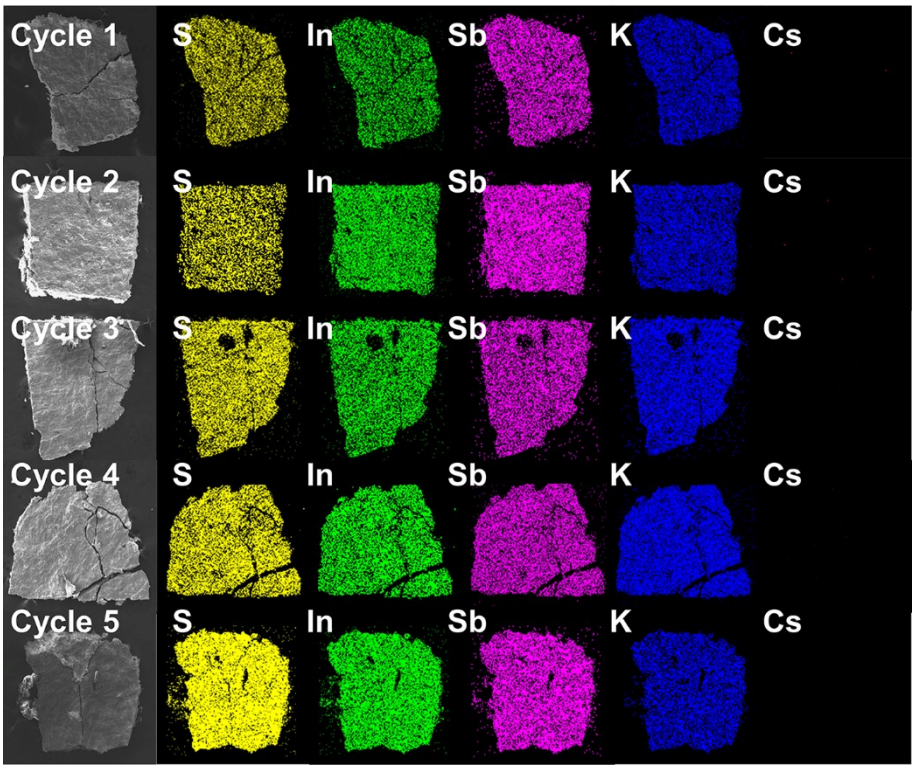

Fig. S7. Mapping analysis of the regenerated KIAS in each cycle (C_0^{Cs} = 53.016 mg/L).

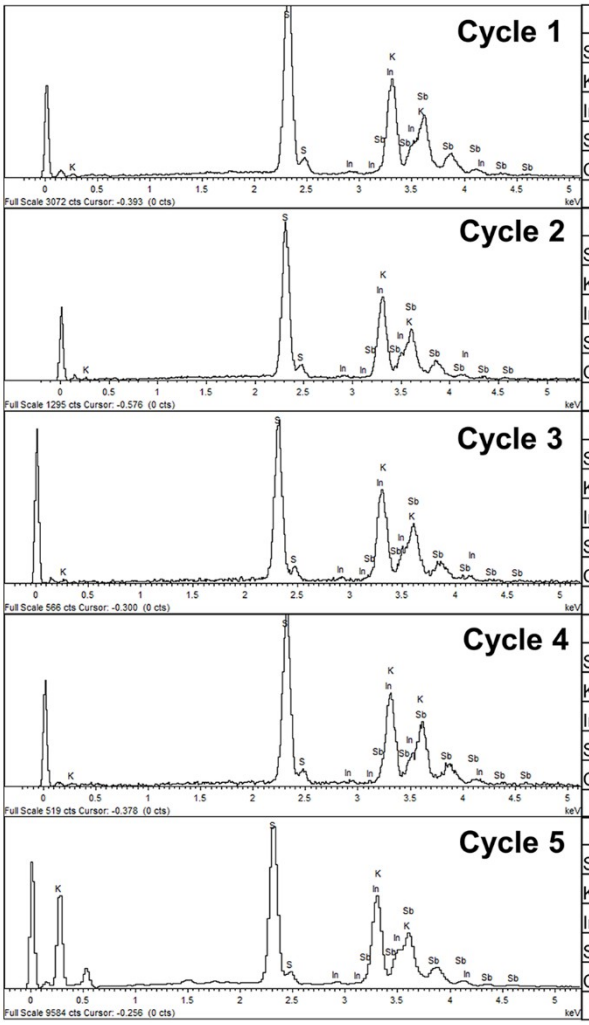

Element	Weight %	Atomic %
S K	31.04	56.37
K K	9.68	14.42
In L	29.81	15.12
Sb L	29.46	14.09
Cs L	0	0
Total	100.00	100.00

Element	Weight %	Atomic %
S K	29.52	55.09
K K	8.93	13.67
In L	33.38	17.4
Sb L	28.16	13.84
Cs L	0	0
Total	100.00	100.00

Element	Weight %	Atomic %
S K	27.64	52.47
K K	9.84	15.32
In L	31.75	16.83
Sb L	30.77	15.38
Cs L	0	0
Total	100.00	100.00

Element	Weight %	Atomic %
S K	28.5	53.9
K K	9.07	14.07
In L	31.09	16.42
Sb L	31.34	15.61
Cs L	0	0
Total	100.00	100.00

Element	Weight %	Atomic %
S K	30.57	55.76
K K	9.87	14.77
In L	29.46	15.01
Sb L	30.1	14.46
Cs L	0	0
Total	100.00	100.00

Fig. S8. EDS results of the regenerated KIAS in each cycle (C_0^{Cs} = 53.016 mg/L).

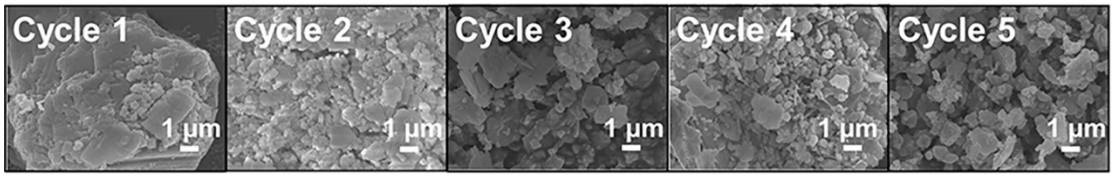

Fig. S9. SEM image of the regenerated KIAS in each cycle (C_0^{Cs} = 53.016 mg/L).

References

1. Y. S. Ho, G. McKay, Pseudo-second order model for sorption processes, *Process Biochem*., 1999, **34**, 451-465.

2. I. Langmuir, The adsorption of gases on plane surfaces of glass, mica and platinum, *J. Am. Chem. Soc.*, 1918, **40**, 1361-1403.

3. H. Freundlich, Über die Adsorption in Lösungen, *Z. Phys. Chem.*, 1907, **57U**, 385-470.

4. H. Faghihian, M. Iravani, M. Moayed and M. Ghannadi-Maragheh, Preparation of a novel PAN-zeolite nanocomposite for removal of Cs^+ and Sr^{2+} from aqueous solutions: Kinetic, equilibrium, and thermodynamic studies, *Chem. Eng. J.*, 2013, **222**, 41-48.

5. M. L. Feng, D. Sarma, Y. J. Gao, X. H. Qi, W. A. Li, X. Y. Huang and M. G. Kanatzidis, Efficient removal of $[UO_2]^{2+}$, Cs^+, and Sr^{2+} ions by radiation-resistant gallium thioantimonates, *J. Am. Chem. Soc.*, 2018, **140**, 11133-11140.

6. B. Zhang, M. L. Feng, H. H. Cui, C. F. Du, X. H. Qi, N. N. Shen, X. Y. Huang, Syntheses, crystal structures, ion-exchange, and photocatalytic properties of two amine-directed Ge-Sb-S compounds, *Inorg. Chem.*,2015, **54**, 8474-8481.

7. C. Yang and K. Cho, Rapid and selective removal of Cs^+ from water by layered potassium antimony thiostannate, *J. Hazard. Mater.*, 2021, **403**, 124105.

8. X. H. Qi, K. Z. Du, M. L. Feng, J. R. Li, C. F. Du, B. Zhang and X. Y. Huang, A two-dimensionally microporous thiostannate with superior Cs^+ and Sr^{2+} ion-exchange property, *J. Mater. Chem. A*, 2015, **3**, 5665-5673.

9. W. A. Li, J. R. Li, B. Zhang, H. Y. Sun, J. C. Jin, X. Y. Huang, M. L. Feng, Layered thiostannates with distinct arrangements of mixed cations for the selective capture of Cs^+, Sr^{2+}, and Eu^{3+} ions, *ACS Appl. Mater. Interfaces*, 2021, **13**, 10191-10201.

10. Y. Y. Liao, J. R. Li, B. Zhang, H. Y. Sun, W. Ma, J. C. Jin, M. L. Feng, X. Y. Huang, Robust and flexible thioantimonate materials for Cs^+ remediation with distinctive structural transformation: A clear insight into the ion-exchange mechanism, *ACS Appl. Mater. Interfaces*, 2021, **13**, 5275-5283.

11. M. J. Manos and M. G. Kanatzidis, Highly efficient and rapid Cs^+ uptake by the layered metal sulfide $K_{2x}Mn_xSn_{3-x}S_6$ (KMS-1), *J. Am. Chem. Soc.*, 2009, **131**, 6599-6607.

12. J. L. Mertz, Z. H. Fard, C. D. Malliakas, M. J. Manos and M. G. Kanatzidis, Selective removal of Cs^+, Sr^{2+}, and Ni^{2+} by $K_{2x}Mg_xSn_{3-x}S_6$ (x = 0.5-1) (KMS-2) relevant to nuclear waste remediation, *Chem. Mater.*, 2013, **25**, 2116-2127.

13. D. Sarma, C. D. Malliakas, K. S. Subrahmanyam, S. M. Islama and M. G. Kanatzidis, $K_{2x}Mg_xSn_{3-x}S_6$ (x = 0.65-1): A new metal sulfide for rapid and selective removal of Cs^+, Sr^{2+} and UO_2^{2+} ions, *Chem. Sci.*, 2016, **7**, 1121-1132.

14. L. Wang, H. Pei, D. Sarrna, X. M. Zhang, K. MacRenaris, C. D. Malliakas, M. G. Kanatzidis, Highly selective radioactive $^{137}Cs^+$ capture in an open-framework oxysulfide based on supertetrahedral cluster, *Chem. Mater.*, 2019, **31**, 1628-1634.

15. H. Yang, M. Luo, L. Luo, H. Wang, D. Hu, J. Lin, X. Wang, Y. Wang, S. Wang, X. Bu, P. Feng and T. Wu, Highly selective and rapid uptake of radionuclide cesium based on robust zeolitic chalcogenide via stepwise ion-exchange strategy, *Chem. Mater.*, 2016, **28**, 8774-8780.

16. E. Rathore, P. Pal and K. Biswas, Reversible and efficient sequestration of cesium from water by the layered metal thiophosphate $K_{0.48}Mn_{0.76}PS_3 \cdot H_2O$, *Chem. Eur. J.*, 2017, **23**, 11085-11092.

17. K. Gupta, B. L. Yuan, C. Chen, N. Varnakavi, M. L. Fu, $K_{2x}Mn_xSn_{3-x}S_6$ (x=0.5-0.95) (KMS-1) immobilized on the reduced graphene oxide as KMS-1/r-GO aerogel to effectively remove Cs^+ and Sr^{2+} from aqueous solution, *Chem. Eng. J.*, 2019, **369**, 803-812.

18. Y. X. Wang, J. R. Li, J.-C. E. Yang, B. L. Yuan, M. L. Fu, Granulous KMS-1/PAN composite for Cs^+ removal, *RSC Adv.*, 2015, **5**, 91431-91435.

19. H. H. Eom, Y. Kim, D. Harbottle, J. W. Lee, Immobilization of KTS-3 on an electrospun fiber membrane for efficient removal of Cs^+ and Sr^{2+}, *J. Environ. Chem. Eng.*, 2021, **9**, 105991.

20. Y. J. Gao, M. L. Feng, B. Zhang, Z. F. Wu, Y. Song and X. Y. Huang, An easily

synthesized microporous framework material for the selective capture of radioactive Cs^+ and Sr^{2+} ions, *J. Mater. Chem. A*, 2018, **6**, 3967-3976.

21. S. Naeimi, H. Faghihian, Performance of novel adsorbent prepared by magnetic metal-organic framework (MOF) modified by potassium nickel hexacyanoferrate for removal of Cs^+ from aqueous solution, *Sep. Purif. Technol.*, 2017, **175**, 255-265.

22. J. Sun, D. Yang, C. Sun, L. Liu, S. Yang, Y. Jia, R. Cai and X. Yao, Potassium niobate nanolamina: A promising adsorbent for entrapment of radioactive cations from water, *Sci. Rep.*, 2014, **4**, 07313.

23. S. Sarina, A. Bo, D. Liu, H. Liu, D. Yang, C. Zhou, N. Maes, S. Komarneni, H. Zhu, Separate or simultaneous removal of radioactive cations and anions from water by layered sodium vanadate-based sorbents, *Chem. Mater.*, 2014, **26**, 4788-4795.

24. P. Amesh, A. S. Suneesh, K. A. Venkatesan, R. U. Maheswari and S. Vijayalakshmi, Preparation and ion exchange studies of cesium and strontium on sodium iron titanate, *Sep. Purif. Technol.*, 2020, **238**, 116393.

25. A. M. El-Kamash, Evaluation of zeolite A for the sorptive removal of Cs^+ and Sr^{2+} ions from aqueous solutions using batch and fixed bed column operations, *J. Hazard. Mater.*, 2008, **151**, 432-445.

26. Y. Kim, Y. K. Kim, J. H. Kim, M.-S. Yim, D. Harbottle, J. W. Lee, Synthesis of functionalized porous montmorillonite via solid-state NaOH treatment for efficient removal of cesium and strontium ions, *Appl. Surf. Sci.*, 2018, **450**, 404-412.

27. Y. Park, Y. C. Lee, W. S. Shin and S. J. Choi, Removal of cobalt, strontium and cesium from radioactive laundry wastewater by ammonium molybdophosphate-polyacrylonitrile (AMP-PAN), *Chem. Eng. J.*, 2010, **162**, 685-695.